Published in final edited form as:
Stem Cells. 2008 March ; 26(3): 611–620. doi:10.1634/stemcells.2007-0429.

Widespread Non-Hematopoietic Tissue Distribution by Transplanted Human Progenitor Cells with High Aldehyde Dehydrogenase Activity

David A. Hess[1], **Timothy P. Craft**[1], **Louisa Wirthlin**[1], **Sarah Hohm**[1], **Ping Zhou**[1], **William C. Eades**[1], **Michael H. Creer**[2], **Mark S. Sands**[1], and **Jan A. Nolta**[1]

[1]Department of Internal Medicine, Division of Oncology, Hematopoietic Development and Malignancy Group, Washington University School of Medicine, St. Louis, MO, USA

[2]Department of Pathology and Laboratory Medicine, St Louis University School of Medicine, Cardinal Glennon Hospital Cord Blood Banking Facility, St Louis, MO, USA

Abstract

Transplanted adult progenitor cells distribute to peripheral organs and can promote endogenous cellular repair in damaged tissues. However, development of cell-based regenerative therapies has been hindered by the lack of pre-clinical models to efficiently assess multiple organ distribution and difficulty defining human cells with regenerative function. After transplantation into beta-glucuronidase (GUSB)-deficient NOD/SCID/MPSVII mice, we characterized the distribution of lineage depleted human umbilical cord blood-derived cells purified by selection using high aldehyde dehydrogenase activity (ALDH) with CD133 co-expression. $ALDH^{hi}$ or $ALDH^{hi}CD133^{+}$ cells produced robust hematopoietic reconstitution, and variable levels of tissue distribution in multiple organs. $GUSB^{+}$ donor cells that co-expressed human (HLA-A,B,C) and hematopoietic ($CD45^{+}$) cell surface markers were the primary cell phenotype found adjacent to the vascular beds of several tissues, including islet and ductal regions of mouse pancreata. In contrast, variable phenotypes were detected in the chimeric liver, with $HLA^{+}/CD45^{+}$ cells demonstrating robust GUSB expression adjacent to blood vessels, and $CD45^{-}/HLA^{-}$ cells with diluted GUSB expression predominant in the liver parenchyma. However, true non-hematopoietic human ($HLA^{+}/CD45^{-}$) cells were rarely detected in other peripheral tissues, suggesting that these $GUSB^{+}/HLA^{-}/CD45^{-}$ cells in the liver were a result of downregulated human surface marker expression *in vivo*, not widespread seeding of non-hematopoietic cells. However, relying solely on continued expression of cell surface markers, as employed in traditional xenotransplantation models, may underestimate true tissue distribution. ALDH-expressing progenitor cells demonstrated widespread and tissue-specific distribution of variable cellular phenotypes,

Correspondence: David A. Hess, PhD, Krembil Centre for Stem Cell Biology, Robarts Research Institute, Room E4-18, 100 Perth Drive, London, Ontario, Canada, N6A 5K8; dhess@robarts.ca; phone: 519-663-4777 (x34152); Fax: 519-663-3789..
AUTHORSHIP Contribution: D.A.H designed and performed research, analyzed data, and wrote the paper. T.P.C performed research and wrote the paper. L.W. performed research. S.H. performed research. W.C.E performed fluorescent activated cell sorting. M.H.C provided umbilical cord blood samples. M.S.S, designed research, provided NOD/SCID MPSVII mice, and edited the manuscript. J.A.N designed research and edited the manuscript.

Current Address: Jan A. Nolta, Ph.D., Professor, Director, Stem Cell Program, University of California at Davis, Room 653, 2425 Stockton Blvd, Sacramento, CA, 95817, Office: 916-453-2335, Fax: 916-453-2173, Jan.nolta@ucdmc.ucdavis.edu

Current Address: David A. Hess, Ph.D., Assistant Professor, Department of Physiology and Pharmacology, University of Western Ontario, Scientist, Vascular Biology Group, Krembil Centre for Stem Cell Biology, Robarts Research Institute, Room 4-18, London, Ontario, Canada, N6A 5K8, Office: 519-663-5777 (x34152), Fax: 519-663-3789, dhess@robarts.ca

Conflict of Interest: The authors declare no conflict of interest.

indicating that these adult progenitor cells should be explored in transplantation models of tissue damage.

Keywords

Transplantation; NOD/SCID model; umbilical cord blood; aldehyde dehydrogenase; CD133

INTRODUCTION

Potentially useful populations of adult stem cells for tissue repair or regenerative medicine include multipotent adult progenitors [1-3], and primitive cells from hematopoietic [4], mesenchymal [5], or endothelial lineages [6]. All of these cell types were first identified in human bone marrow (BM) but several are also present in human umbilical cord blood (UCB) [7-10]. In the context of regenerative therapies, the contribution of adult stem cells is not limited to direct replacement of damaged cells. Introduction of transplanted adult cells can enhance survival, induce proliferation, and improve the function of damaged recipient cells in neural [11,12], cardiac [13-15], and endocrine tissues [16,17]. Therefore, transplanted hematopoietic [18-20], mesenchymal [15,21], or endothelial progenitors [14,22], from BM or UCB, may orchestrate the co-ordinated release of pro-angiogenic or pro-survival factors, resulting in improved cellular function. Regardless of the exact mechanism of tissue repair, the prospective isolation of human cells with documented regenerative function after transplantation has proven difficult due to the lack of sensitive models to detect tissue residence, particularly in solid organs.

While human hematopoietic and endothelial progenitors can be identified by clonogenic assays *in vitro*, whether these cells seed and survive in peripheral tissues after transplantation *in vivo* is not well described. We have previously identified putative mixed progenitor populations according to conserved cytosolic aldehyde dehydrogenase (ALDH) activity [23], with or without further purification using CD133 expression, a cell surface marker expressed on hematopoietic and endothelial progenitors [24,25]. Cytosolic ALDH is an enzyme highly expressed in hematopoietic progenitors [26], and implicated in the resistance of hematopoietic progenitor cells to alkylating agents [27]. Transplantation of lineage depleted (Lin^-), ALDH-expressing cells into immune deficient NOD/SCID mice produces robust, multilineage reconstitution in hematopoietic organs [23,24]. To further characterize the distribution and survival of these progenitor cells in multiple tissues, we intravenously transplanted UCB-derived $ALDH^{lo/hi}$ and $ALDHhiCD133^{-/+}$ cells into NOD/SCID/MPSVII mice, a model designed to accurately document donor/recipient cell interactions in peripheral tissues.

β-glucuronidase (GUSB) is a lysosomal enzyme that is ubiquitously expressed. GUSB deficiency results in the lysosomal storage disease, mucopolysaccharidosis type VII (MPSVII) [28], characterized by skeletal dysplasia, mental retardation, and reduced lifespan. GUSB-deficient mice [29], have been used to study disease progression and the localization of various transplanted murine cell types [30-34]. By crossing the MPSVII mutation onto the NOD/SCID background [35], transplanted human cells can be readily visualized by virtue of their GUSB activity without reliance on the persistent expression of human-specific cell surface markers.

In this study, we employed the NOD/SCID/MPSVII model to characterize the ability of human ALDH-expressing populations to reconstitute hematopoiesis and disseminate to non-hematopoietic tissues. After transplantation, ALDH-expressing cells were widely trafficked peripheral organs and demonstrated variable distribution patterns. Human $GUSB^+$ donor

cells co-expressing hematopoietic (CD45) cell surface markers were the primary cell phenotype in vascular beds of organs, including the islet and ductal regions of mouse pancreata. Variable donor cell phenotypes were detected in the chimeric liver, with $GUSB^+$ cells demonstrating reduced expression of both human and hematopoietic cell surface markers, indicating more widespread tissue distribution after xenotransplantation than had been previously detected.

MATERIALS AND METHODS

NOD/SCID/MPSVII mice

The NOD/SCIDMPSVII mouse was produced by M.S.S at Washington University School of Medicine (St. Louis, MO) by 10 backcrosses of the MPSVII mutation from its original strain (B6.C-H-2^{bml}) onto the NOD/SCID mouse background (both mice from Jackson Laboratories [35]). Experimental NOD/SCID/$MPSVII^{-/-}$ mice, bred in our colony at Washington University in compliance with all regulatory committees, were identified by a GUSB-sequence specific PCR assay, and confirmed by a lack of GUSB activity as previously described [35,36]. Human cell reconstitution after the transplantation of human MSC, UCB-derived or mobilized peripheral blood-derived $CD34^+$ cells into NOD/SCID/MPSVII mice has been previously detailed [35,37], with repopulating frequencies equivalent to the parental immune deficient NOD/SCID mice.

Human Cell Purification by Aldehyde Dehydrogenase Activity

Human UCB samples were obtained from the cord blood banking facility at Cardinal Glennon Children's Hospital, St. Louis, MO, and used in accordance with local ethical and biohazard authorities at Washington University School of Medicine, St. Louis, MO. UCB samples were diluted with phosphate-buffered saline (PBS), and MNC were isolated by Hypaque-Ficoll centrifugation (Pharmacia Biotech, Uppsala, Sweden). MNC were depleted of contaminating erythrocytes by red blood cell lysis in 0.8% ammonium chloride solution (Stem Cell Technologies, Vancouver, BC, Canada). Human UCB MNC were enriched for lineage depleted (Lin^-) cells by magnetic bead separation, as previously described [23,24]. The resulting Lin^- population was further purified based on ALDH activity by staining with Aldefluor™ substrate (StemCo Biomedical, Durham, NC) according to the manufacturer's specifications. This fluorescent substrate is metabolized by cytosolic ALDH, and retained within the cells due to its negative charge [23,26], and $ALDH^{lo}Lin^-$ or $ALDH^{hi}Lin^-$ cells were selected by FACS (MoFlo; Cytomation, Denver, CO). Alternatively, Lin^- cells were also co-stained with anti-human CD133-APC (Miltenyi Biotec, Auburn, CA) after incubation with the Aldefluor™ substrate, and $ALDH^{hi}CD133^-Lin^-$ or $ALDH^{hi}CD133^+Lin^-$ cells were selected by FACS. Cell populations were routinely isolated to >95% purity and >95% viability by Trypan blue staining, and were screened for CD34 and CD45 (all antibodies BD) expression by flow cytometry.

Transplantation of Purified Cell Populations into NOD/SCID/MPSVII Mice

Unsorted Lin^-, $ALDH^{lo}Lin^-$, $ALDH^{hi}Lin^-$, $ALDH^{hi}CD133^-Lin^-$, or $ALDH^{hi}CD133^+Lin^-$ cells were transplanted by tail vein injection into 8-12 week old, sublethally irradiated (300cGy) NOD/SCID/$MPSVII^{-/-}$ mice. NOD/SCID/MPSVII mice transplanted with PBS served as controls for analysis by flow cytometry and histochemical staining.

Analysis of Human Cell Distribution in the Tissues of Transplanted Mice

BM was flushed from the marrow compartments with PBS supplemented with 2% FCS. Spleen, liver, lung and pancreas were mechanically dissociated without enzymatic digestion, sequentially filtered, and resuspended in PBS/2% FCS. Peripheral blood was collected from

anaesthetized mice by retro-orbital eye bleed as described previously [23]. BM and peripheral blood were lysed with a 0.8% ammonium chloride solution (Stem Cell Technologies). For FACS analysis, approximately 10^6 suspended cells were incubated with blocking solution and monoclonal antibodies for the human pan-leukocyte specific marker CD45 in combination with HLA-A,B,C, or isotype controls (all antibodies Becton Dickinson (BD), San Jose, CA). Dissociated solid tissues (liver, lung and pancreas) were also co-stained with a viability marker, 7-AAD (BD) immediately before analysis, in order to exclude cells damaged by processing. Cells were analyzed by 3-color flow cytometry on a Coulter FC-500 flow cytometer (Beckman-Coulter, Miami, FL). For flow cytometric analysis of GUSB positivity, dissociated cells from mouse spleen, liver, or pancreas were incubated with 100μM ImaGene Green C12-FDGlcU GUSB substrate (Molecular Probes, Eugene, OR) for 1-2 hours at 37°C. Cells were co-stained with anti-human CD45-APC or APC-isotype control and assayed by FC-500 as described above.

GUSB-Specific Histochemical Assay

Liver, spleen, lung, pancreas, heart, kidney, brain, eye, skeletal muscle, sternum, and hip from NOD/SCID MPSVII were frozen in optimal cutting temperature (OCT) embedding medium (Sakura, Torrance, CA) for histochemical analysis. Serial sections were taken at 10μm thickness and stained for GUSB activity as described previously using naphthol-AS-BI-β-D-glucuronide (ASBI, Sigma, St Louis, MO) as a substrate [38,39]. Slides were counterstained with methyl green.

Immunohistochemistry

Frozen sections from transplanted NOD/SCID/MPSVII mouse spleen, liver and pancreas were fixed for 15 minutes in acetone at 4°C and blocked at room temperature with mouse-on-mouse reagent (Vector Labs, Burlingame, CA) [35]. Unconjugated mouse anti-human CD45 primary antibody (anti-Hle-1, BD) diluted 1/200 was conjugated with an alkaline phosphatase goat anti-mouse IgG antibody (Sigma) followed by alkaline phosphatase development reagents (Vector Labs). Adjacent sections were sequentially immunostained for CD45 and GUSB activity as described above in order to detect donor derived $GUSB^+$ cells that co-express CD45.

RESULTS

Isolation of purified human populations

Increased ALDH activity is a characteristic of cells that possess documented neural and hematopoietic progenitor function *in vivo* [23,26,40,41]. We have previously described the purification of UCB Lin^- cells according to ALDH activity by FACS with the $ALDH^{lo}$ and $ALDH^{hi}$ populations comprising 31.5±1.8% and 50.1±2.4% of total Lin^- cells respectively [23]. Since endothelial progenitors can augment vascular regeneration (for review see [42]), and because CD133-expression is also conserved on progenitor cells from endothelial, hematopoietic, and neural lineages [9,43-45], $ALDH^{hi}Lin^-$ cells were further purified based on CD133 expression. As previously described [24],$CD133^-$ and $CD133^+$ cells represented 33.7±1.7% and 50.4±2.5% of $ALDH^{hi}Lin^-$ cells, or 14.7±2.1% and 23.2±4.3% of the total Lin^- cells, respectively. CD34 expression on the cells used in this study were similar to previous reports ($ALDH^{lo}Lin^-$ cells=34.3±8.3% $CD34^+$, $ALDH^{hi}Lin^-$ cells = 87.5±13.7% $CD34^+$, $ALDH^{hi}CD133^-Lin^-$ cells = 75.4±7.5% $CD34^+$, $ALDH^{hi}CD133^+Lin^-$ cells = 92.7±5.4% $CD34^+$, and Lin− = 55.4±9.8 $CD34^+$) [23,24]. Starting populations demonstrated >95% expression of the pan leukocyte marker CD45 by FACS (data not shown), indicating that UCB ALDH-expressing progenitors were primarily hematopoietic in origin.

Detection of donor cell tissue distribution after transplantation of ALDH-expressing populations

Purified human $ALDH^{lo}Lin^{-}$, $ALDH^{hi}Lin^{-}$, $ALDH^{hi}CD133^{-}Lin^{-}$, and $ALDH^{hi}CD133^{+}Lin^{-}$ cells ($0.5\text{-}4\times10^{5}$ cells) were transplanted into NOD/SCID/MPSVII mice following 300 cGy radiation, without co-transplantation of supportive accessory cells [23,46]. Human HLA-A,B,C (HLA, ubiquitously expressed on human nucleated cells) and CD45 (pan-leukocyte marker) co-expression were used to differentiate hematopoietic ($HLA^{+}/CD45^{+}$) from non-hematopoietic ($HLA^{+}/CD45^{-}$) human cell detection by FACS (Fig. 1). Dead cells (7-AAD+) and debris were excluded from the analysis of liver and pancreas (data not shown).

Intravenous injection of $2\times10^{5}ALDH^{hi}Lin^{-}$ cells produced a high frequency (74.4±7.9%, n=4) of human hematopoietic ($HLA^{+}/CD45^{+}$) reconstitution in NOD/SCID/MPSVII mouse BM, analyzed 5-6 weeks post-transplantation (Fig. 1A). An equal dose of $ALDH^{hi}CD133^{+}Lin^{-}$ cells (Fig. 1D) reconstituted the BM at a significantly ($p<0.05$) reduced level (25.6±10.4%, n=4). Corresponding $ALDH^{lo}Lin^{-}$ (Fig. 1A inset, n=3) and $ALDH^{hi}CD133^{-}Lin^{-}$ (Fig. 1D inset, n=3) cells were not detected in the BM or any other tissue. For comparison, transplantation of 2×10^{5} unfractionated Lin^{-} cells produced 19.0±7.0% (n=3) human cell repopulation at 5-6 weeks post-transplantation (data not shown). Both $ALDH^{hi}Lin^{-}$ and $ALDH^{hi}CD133^{+}Lin^{-}$ cells also demonstrated consistent seeding in the liver and pancreas (Fig. 1B, C, E, and F). As detected by flow cytometry to assess cell surface markers, cells seeding these tissues appeared to be primarily hematopoietic in origin, as non-hematopoietic ($HLA^{+}/CD45^{-}$) cells were rarely detected in tissues using this particular assay (Fig. 1).

We transplanted a total of 46 NOD/SCID/MPSVII mice with $0.5\text{-}4\times10^{5}$ $ALDH^{hi}Lin^{-}$, $ALDH^{lo}Lin^{-}$, $ALDH^{hi}CD133^{+}Lin^{-}$, or $ALDH^{hi}CD133^{-}Lin^{-}$ cells and quantified human cell chimerism by FACS in the BM (Fig. 2A), peripheral blood (Fig. 2B), liver (Fig. 2C), and pancreas (Fig. 2D). Human $ALDH^{hi}Lin^{-}$ cells produced prolonged hematopoietic reconstitution in the BM of all transplanted mice at 5-6 (59.1±7.8% $HLA^{+}/CD45^{+}$, n=11) and at 10-12 weeks (66.0±5.0% $HLA^{+}/CD45^{+}$, n=8) post-transplantation (Fig. 2A). In contrast, transplanted $ALDH^{lo}Lin^{-}$ cells demonstrated little or no reconstituting ability, with only 2 of 11 mice demonstrating <0.3% human cells after the injection of as many as 4×10^{5} cells. Highly purified $ALDH^{hi}CD133^{+}Lin^{-}$ cells repopulated the murine BM at approximately 3-fold lower levels ($p<0.05$) compared to $ALDH^{hi}Lin^{-}$ progenitors (Fig. 2A). Transplanted $ALDH^{hi}CD133^{-}Lin^{-}$ cells did not engraft. Transplantation of $ALDH^{hi}Lin^{-}$ (n=3) and $ALDH^{hi}CD133^{+}Lin^{-}$ (n=3) cells yielded primarily myeloid and B-lymphoid progeny (data not shown). Stable, multilineage hematopoietic repopulation was established in mice transplanted with ALDH-expressing cells, providing a potential reservoir of human cells for dispersal to peripheral tissues.

Established hematopoietic chimerism established the transit of human cells in the peripheral blood of transplanted mice. Thus, high BM reconstitution by transplanted $ALDH^{hi}Lin^{-}$ cells led to consistent detection of human cells in the peripheral blood at 5-6 (13.4±6.0% $HLA^{+}/CD45^{+}$, n=11) and at 10-12 (12.9±6.8% $HLA^{+}/CD45^{+}$, n=8) weeks post-transplantation (Fig. 2B). After transplantation of $ALDH^{hi}CD133^{+}Lin^{-}$ cells, human progeny were detected at lower levels in the peripheral blood at 5-6 (2.8±1.5% $HLA^{+}/CD45^{+}$, $p<0.01$) and at 10-12 (0.4±0.1% $HLA^{+}/CD45^{+}$, $p<0.05$) weeks post-transplantation, suggesting lowered BM chimerism reduced trafficking of human cells via the murine circulation.

Compared to BM and peripheral blood, lower levels of human cells were observed by FACS in the liver (Fig. 2C) and pancreas (Fig. 2D) of NOD/SCID/MPSVII mice transplanted with $ALDH^{hi}Lin^{-}$ or ALDHhi$CD133^{+}Lin^{-}$ cells. For all transplanted cell populations, the

frequency of human cells in the liver was approximately 5-fold higher than in the pancreas (Fig. 2C, D). Human cell detection in these tissues was consistently higher after transplantation of $ALDH^{hi}Lin^{-}$ cells, as compared to $ALDH^{hi}CD133^{+}Lin^{-}$ cells. Taken together, these data suggest that increased hematopoietic chimerism led to increased peripheral tissue seeding, and that human cells were distributed to various peripheral tissues via the circulation at variable frequencies after intravenous transplantation.

Distribution of $GUSB^{+}$ cells in the tissues of transplanted NOD/SCID/MPSVII mice

The major advantage of the NOD/SCID/MPSVII model employed in these studies is the sensitive detection of $GUSB^{+}$ donor cells in tissues without reliance on the continued expression of human cell surface markers or *in situ* hybridization [35]. In addition, cell phenotype, and distinct human cell localization within solid tissues, and interaction with recipient cells can also be documented by microscopy, without the use of FACS. Figure 3 shows the representative distribution of $GUSB^{+}$ cells *in situ* for mice injected with $ALDH^{lo}Lin^{-}$ (A), $ALDH^{hi}Lin^{-}$ (B), or $ALDH^{hi}CD133^{+}Lin^{-}$ (C) cells in the spleen, liver, and pancreas at 6 weeks post-transplantation. Tissues from NOD/SCID/MPSVII mice not transplanted with human cells (PBS-injected) were completely devoid of GUSB staining (data not shown). Mice injected with non-repopulating $ALDH^{lo}Lin^{-}$ (Fig. 3A) cells showed only rare $GUSB^{+}$ cells in spleen (arrow, Fig. 3A), liver or pancreas. Consistent with flow cytometric data, $ALDH^{hi}CD133^{-}Lin^{-}$ cells or related progeny were not detected in any analyzed tissues by GUSB histochemical expression (data not shown). In contrast, widespread distribution of GUSB+ donor cells was observed in tissues from $ALDH^{hi}Lin^{-}$ (Fig. 3B) and $ALDH^{hi}CD133^{+}Lin^{-}$ transplanted mice (Fig. 3C). As shown in Figure 4, high levels of human cell dispersal via the peripheral circulation were observed 6-weeks after intravenous injection of $ALDH^{hi}Lin^{-}$ cells in a highly reconstituted (66.5% human HLA^{+}/$CD45^{+}$ cells in murine BM) representative mouse. Notably, $GUSB^{+}$ human cells could be found in nearly all tissues examined, suggesting that transplanted $ALDH^{hi}Lin^{-}$ progenitors from UCB display more widespread distribution in peripheral tissues than previously recognized [23,24].

After transplantation of 2×10^{5} $ALDH^{hi}Lin^{-}$ cells, donor-derived $GUSB^{+}$ cells were abundant in hematopoietic tissues such as the sternum marrow (Fig. 4A) and spleen (Fig. 4B). Transplanted mice that produced more modest murine BM repopulation, showed clustering of $GUSB^{+}$ cells along the endosteal surface of the bone, the site of primitive progenitor adhesion within the BM [47,48]. Transplanted human $ALDH^{hi}Lin^{-}$ cells uniformly infiltrated highly vascular tissues such as the liver (Fig. 4C), and lung (Fig. 4D), whereas kidney (Fig. 4E), cardiac muscle (Fig. 4F), and cartilage (Fig. 4G) showed less dense scattered distribution. Patterned distribution by $ALDH^{hi}Lin^{-}$ cells was observed in the pancreas, with donor derived $GUSB^{+}$ cells selectively found neighboring both ductal and islet regions but not highly represented in exocrine areas (Fig. 4H). Scattered $GUSB^{+}$ cells were present at reduced intervals in the brain (Fig. 4I), and in close association with the retinal pigment epithelial layer of the eye (Fig. 4J). A similar pattern of GUSB-expressing cells was observed at 5-6 and 10-12 weeks post-transplantation. Mice transplanted with $ALDH^{hi}CD133^{+}Lin^{-}$ cells demonstrated a similar pattern of distribution, albeit with proportionately fewer cells (data not shown).

Transplanted human $ALDH^{hi}Lin^{-}$ cells localized to ductal and islet regions in the pancreas

Tissues such as the liver and pancreas may provide amenable targets for the development of cell and gene therapy applications. Distinct, patterned distribution of human ALDH-expressing progenitors ($ALDH^{hi}Lin^{-}$ and $ALDH^{hi}CD133^{+}Lin^{-}$ cells) was consistently observed in the pancreas of transplanted NOD/SCID/MPSVII mice (Fig. 5). Specificly, $GUSB^{+}$ cells or progeny were consistently detected adjacent to ductal (Fig. 5A) and islet

(Fig. 5B) structures in the proximal portion of the endocrine pancreas. $GUSB^+$ donor cells clearly surrounded the borders of islet structures (Fig. 5B). This distribution was observed in all pancreata examined by GUSB histochemistry (n=4, for $ALDH^{hi}Lin^-$ transplants). Donor-derived $GUSB^+$ cells located in both ductal and islet regions consistently co-stained with human CD45 (Fig. 5C), indicating that these cells were primarily hematopoietic in origin. The arrows in Figure 5D clearly mark $CD45^+$ (brown) and $GUSB^+$ (red) donor-derived cells, confirming flow cytometric data that human cells in the pancreas were primarily hematopoietic. Furthermore, this distribution occurred without prior chemical damage to beta cells and did not result in obvious inflammation. Insulin staining and control of blood glucose in these mice were normal prior to and throughout the post-transplantation period (data not shown).

Characterization of donor cells detected in the liver

Since the fusion of mouse and human BM cells with murine hepatocytes after xenotransplantation has been established [49,50], and because preliminary GUSB screening in the liver suggested more widespread human cell residence than predicted by FACS (Fig. 1B), we further investigated the phenotypes of cells detected in the liver (Fig. 6). Representative photomicrographs of representative liver sections from chimeric mice transplanted with human UCB $ALDH^{hi}Lin^-$ cells at low (Fig. 6A, 100×) and high (Fig. 6B, 400×) demonstrated the diffuse dispersal of human cells throughout the liver, and also visualize the cytoplasmic localization of GUSB staining in donor-derived human cells ranging in size from 5μm to >20μm diameter. The majority of human cells detected within liver tissue 5-6 weeks post-transplantation were hematopoietic (CD45+) (Fig. 6C) in origin, and co-expressed mature lineage markers for human myeloid cells ($CD45^+CD33^+$, Fig. 6D), human B-lymphocytes ($CD45^+CD19^+$, Fig. 6E), and human macrophages ($CD45^+CD11b^+$, Fig. 6E). Although these analyses were performed without tissue perfusion prior to euthanasia to remove blood vessel resident hematopoietic cells, these data demonstrate the widespread distribution of donor hematopoietic cells with access to a hepatic microenvironment. Other highly vascularized tissues such as the myocardium (Fig. 4F), and neural tissue (Fig. 4I) did not achieve such widespread donor cell distribution.

At 10-12 weeks post-transplantation, two distinct donor-derived cell phenotypes demonstrating different morphology and intensity of GUSB-staining, were distributed throughout the livers of mice transplanted with either $ALDH^{hi}Lin^-$ (Fig. 7A, B) or $ALDH^{hi}CD133^+Lin^-$ (Fig. 7C, D) cells at 10-12 weeks post-transplantation. Other tissues such as the lung (Fig. 4D) and kidney (Fig. 4E) also showed varying intensities of GUSB expression in donor cells, whereas GUSB intensities were consistently high in individual cells detected within the pancreas (Fig. 4G), brain (Fig. 4I) and eye (Fig. 4J). Although different cell types can vary in their expression of endogenous GUSB, cells detected in the livers of transplanted mice revealed the presence of small, round, intensely red stained cells (Fig. 7A-C, arrowheads), and larger, moderately red stained cells (Fig. 7A-D, arrows) throughout the liver. These larger, moderately stained donor cells were present in mouse livers at 5-6 weeks and 10-12 weeks post-transplantation.

Flow cytometric analysis of dissociated liver tissue at 10-12 weeks after transplantation with $ALDH^{hi}Lin^-$ cells revealed a relatively high frequency of cells (R1, 15.0±4.9%) that metabolized a fluorescent substrate of GUSB (Fig. 7E). In contrast, these mice (n=4) showed low frequencies of human HLA-A,B,C (0.9±0.5%) and CD45 (0.7±0.4%) cell surface expression by flow cytometry (Fig. 7F). Dual color flow cytometry for GUSB activity and human cell surface CD45 expression, revealed a small but distinct cluster of cells intensely stained for GUSB activity that co-express human cell surface CD45 (1.1±0.6% $GUSB^{hi}CD45^+$), and a larger population of donor-derived, GUSB-expressing cells (13.4±4.5%) with reduced expression of CD45 (Fig. 7G). The $CD45^+$ cells always co-

expressed human HLA-A,B,C, whereas human HLA-A,B,C expression was not detected on any $CD45^{-}$ cells detected in the liver (data not shown), suggesting that both human HLA-A,B,C and CD45 expression was reduced by donor-derived cells within the murine liver. $CD45^{-}$ cells were not evident in other non-hematopoietic tissues such as pancreas (Fig. 5C), where there was concordance between CD45 and GUSB staining. In addition, $CD45^{-}$ cells were not observed in previous studies of human UCB $CD34^{+}$ cell transplantation in the NOD/SCID/MPSVII model by Hofling et al, where liver-resident cells always co-expressed CD45 [35]. Thus, donor cells in the liver of mice transplanted with $ALDH^{hi}Lin^{-}$ cells revealed more variable phenotypes than previously realized with Lin− or $CD34^{+}$ cells.

To further confirm these findings, serial sections from livers were stained for CD45 expression alone (Fig. 7H), or co-stained to detect GUSB activity (red) and CD45 (brown) expression in the same cell (Fig. 7I). Cells expressing human CD45 were rarely found dispersed through the liver parenchyma, however occasional clusters of $CD45^{+}$ cells were observed in perivascular regions (Fig. 7H, I). Numerous $GUSB^{+}$ cells that did not express human CD45 (Fig. 7I, arrowheads) were observed throughout the liver. These liver-resident $GUSB^{+}CD45^{-}$ cells were more numerous at 10-12 weeks post-transplantation, were widely dispersed, in close contact with murine hepatocytes, and were distinct from the $GUSB^{+}CD45^{+}$ human cells within liver blood vessels (Fig. 6 and 7). Thus, detection of GUSB-expression using the NOD/SCID/MPSVII model provides a unique method to detect these persistent donor-derived cells within non-hematopoietic tissues.

In order to uncover the identity or lineage-restriction of CD45- donor cells detected within the liver, we stained serial sections for human hepatocyte-specific albumin expression using immunofluorescence (Fig 7J), followed by routine GUSB-expression using colormetric immunohistochemistry (Fig. 7K). This analysis revealed the presence of rare clusters and individual human cells that possess a human albumin expression, a well-documented hepatocyte-specific function *in vivo* (arrows) [49,50]. However, the majority of donor derived $GUSB^{+}$ human cells did not co-stain for human albumin (arrowheads, n=3), suggesting that some but not all liver resident progeny of UCB $ALDH^{hi}Lin^{-}$ cells possessed the capacity to adopt typical hepatocyte morphology and function after intravenous transplantation, hematopoietic reconstitution, and transport to the liver via the peripheral circulation.

DISCUSSION

Highly enriched human UCB-derived cells expressing high ALDH activity demonstrated robust hematopoietic reconstitution and efficient dissemination to multiple peripheral tissues of transplanted NOD/SCID/MPSVII mice via the peripheral circulation. Hematopoietic reconstitution by the $ALDH^{hi}Lin^{-}$ population in the BM and spleen exceeded both unfractionated Lin^{-} cells and further purified $ALDH^{hi}CD133^{+}Lin^{-}$ population after transplantation of equal cell doses, and confirmed the strong hematopoietic repopulating function of ALDH-expressing cells from UCB [23,24]. We have previously reported that the $ALDH^{hi}CD133^{+}$ population contained a higher SCID repopulating cell (SRC) frequency when compared to more heterogeneous $ALDH^{hi}Lin^{-}$ cells when transplanted into immune deficient recipients at limiting dilution [24]. Although fewer $ALDH^{hi}CD133^{+}Lin^{-}$ cells are able to establish hematopoiesis in NOD/SCID and NODSCID beta-2 microglobullin null mice, this highly purified population actually induced less robust repopulation, primarily due to the removal of accessory cells that support the efficient proliferation and expansion of $ALDH^{hi}$ SRC. A similar phenomenon has been previously reported when comparing BM-chimerism by $CD34^{+}$ and $CD34^{+}CD38^{-}$ cells transplanted without accessory cell support [7,46,51]. Nonetheless, stable BM reconstitution was achieved by each cell population within 6 weeks post-transplantation and remained so for at least 12 weeks. Increased levels

of human hematopoietic reconstitution led to increased transit of human cells in the peripheral circulation and increased detection of donor cells in tissues. Thus, strong hematopoietic repopulation and widespread tissue dispersal underscore the potential of human ALDH-expressing progenitor populations in the future development of cellular therapies for hematopoietic replacement and/or tissue repair.

Established human cell chimerism in the murine BM following transplantation, initiated increased trafficking of human cell progeny within the peripheral circulation. In turn, donor cell distribution to tissues rich in capillary beds such as the lung and the liver was increased when compared to less vascularized tissues. Thus, increased tissue perfusion may lead to efficient exposure of potentially regenerative cells to diseased or damaged tissues. However, widespread distribution of non-hematopoietic, human albumin expressing cells in the liver can not be fully explained by the initial seeding of cells in the microvasculature alone because other highly vascularized tissues such as the brain and myocardium do not demonstrate increased human cell distribution and variation in phenotype. In addition, quantitative detection by GUSB-expressing donor cells by FACS in the livers of chimeric animals at 10-12 weeks post-transplantation routinely outweighed the frequency human cells detected by human CD45 or human HLA A,B,C expression in the circulation, suggesting the accumulation of human cells that did not express human hematopoietic markers specifically in the liver.

Detailed analysis of tissue-resident cell phenotype revealed selective detection of human hematopoietic cells in vascular regions of tissues including the endocrine pancreas surrounding both ducts and islets. Immediate and persistent transit of these cells to the pancreatic microenvironment may be important for the regeneration of beta cell function after streptozotocin treatment, as murine and human BM-derived progenitor cells have been shown to initiate proliferation and restore insulin content in hyperglycemic recipients [16,17]. Thus, human ALDH-expressing cells represent putative progenitors with endocrine-delivery characteristics necessary for potential endogenous regeneration of damaged pancreatic tissue. Future experiments will address the potential of these cells for tissue repair.

The GUSB deficiency in our NOD/SCID/MPSVII model allowed for specific and sensitive detection of donor-derived, $GUSB^+$ cells. In most tissues, including the BM, spleen, and pancreas, detectable GUSB activity correlated closely with human HLA-A,B,C and CD45 cell surface marker expression. However, flow cytometric detection of intracellular GUSB activity combined with human cell surface marker detection in the liver revealed GUSB positive cells with low expression of human CD45. However, since the starting ALDH-expressing populations were >95% $CD45^+$, and since $HLA^+/CD45^-$ cells were rare in other tissues, our data suggests that $GUSB^+/HLA^-/CD45^-$ cells in the liver, may be the result of an overall reduction in human cell surface marker expression to the point where human HLA–A, B, C and CD45 were not detected in cells with considerable GUSB expression. GUSB-expression within the liver was also distinct and confined within the membrane boundaries of cells with a hepatocyte morphology, indicating that the potential uptake of GUSB enzyme by murine hepatocytes by a phenomenon known as cross-correction was not observed as previously reported for transplanted CD34 cells [35]. In that report, there was a perfect concordance between CD45 and GUSB expression in the liver after transplantation of human CD34+ cells into the NOD/SCID/MPSVII mouse. These data demonstrated that human cells that express physiological levels of GUSB do not contribute sufficient enzyme to surrounding cells to be detected histochemically. Cross-correction to murine cells is also unlikely in the current studies, because in order for a GUSB- murine cell to endocytose enough enzyme to be detected histochemically, a cell expressing high levels would need to be nearby. This is clearly not the case (Fig. 7D and 7E).

Cellular fusion between hematopoietic cells and hepatocytes has been well documented by several groups [49,50,52]. Furthermore, murine BM cell mobilization or human UCB cell transplantation in models of murine hepatic damage after CCl_4 administration, have demonstrated that these hematopoietic cells can undergo cell fusion events *in vivo* [53,54]. Thus, in our system that did not employ chemical-induced hepatocyte damage, the presence of moderate GUSB activity in $CD45^-$ cells of the liver may have occurred via cellular fusion and nuclear reprogramming, resulting in the dilution of GUSB activity and the downregulation of human cell surface marker expression, and possible upregulation of human albumin production (Fig. 7J, K). However, we cannot rule out the possibility that donor UCB-derived non-hematopoietic ($CD45^-$) cells, namely putative mesenchymal or endothelial progenitors, that also demonstrate reduced expression of human HLA but lacked the expression of human albumin (Fig. 7), may have established residence specifically in murine liver [37]. In previous studies, transplanted human $CD34^+$ cells did not demonstrate reduced human CD45 expression in the liver of NOD/SCID/MPSVII mice [35], indicating that this expression pattern may be unique to ALDH-expressing cells or circulating progeny. Regardless of lineage restriction, these liver resident cells were donor-derived ($GUSB^+$), and the use of traditional models to detect tissue residence after transplantation, that solely relied on the continued expression of cell surface markers, may have underestimated donor cell distribution in peripheral organs.

In summary, ALDH-expressing populations from human UCB are an easily procured, rich source of repopulating multipotent progenitors for a variety of potential clinical cellular transplantation applications. Although ALDH cells from UCB are comprised primarily of hematopoietic progenitors [23-26], ALDH-expressing cells from alternate adult sources such as human BM may also contain enriched mesenchymal, or endothelial progenitors [55], recently implicated in important regenerative processes [16,17]. The diverse localization, variable donor cell phenotypes, and distinct distribution patterns characteristic of this population have not been previously described for intravenously transplanted progenitors. The ability of ALDH-expressing cells to distribute to multiple organs after transplantation provides an efficient means to deliver primitive progenitor cells to potentially mediate regenerative processes after tissue damage.

Acknowledgments

The authors wish to thank Jackie Hughes for flow cytometer operation, Marie Roberts for assistance with GUSB staining, and Krysta Levac for critical review of the manuscript.

This work was supported by grants from the National Institutes of Health to J.A.N. (NIDDK; R01DK61848-01 and NHLBI; R01HL073256-01), to M.S.S. (NIDDK; R01DK57586), and from the Krembil Foundation and the Juvenile Diabetes Research Foundation to D.A.H (Regeneration of β-cell Function Initiative, RBCF; #1-2005-1173).

REFERENCES

1. Jiang Y, Jahagirdar BN, Reinhardt RL, et al. Pluripotency of mesenchymal stem cells derived from adult marrow. Nature Jul 4;2002 418(6893):41–49. [PubMed: 12077603]
2. Reyes M, Dudek A, Jahagirdar B, Koodie L, Marker PH, Verfaillie CM. Origin of endothelial progenitors in human postnatal bone marrow. J Clin Invest Feb;2002 109(3):337–346. [PubMed: 11827993]
3. Schwartz RE, Reyes M, Koodie L, et al. Multipotent adult progenitor cells from bone marrow differentiate into functional hepatocyte-like cells. J Clin Invest May;2002 109(10):1291–1302. [PubMed: 12021244]
4. Kondo M, Wagers AJ, Manz MG, et al. Biology of hematopoietic stem cells and progenitors: implications for clinical application. Annu Rev Immunol 2003;21:759–806. [PubMed: 12615892]

5. Prockop DJ. Marrow stromal cells as stem cells for nonhematopoietic tissues. Science Apr 4;1997 276(5309):71–74. [PubMed: 9082988]
6. Asahara T, Murohara T, Sullivan A, et al. Isolation of putative progenitor endothelial cells for angiogenesis. Science Feb 14;1997 275(5302):964–967. [PubMed: 9020076]
7. Bhatia M, Wang JC, Kapp U, Bonnet D, Dick JE. Purification of primitive human hematopoietic cells capable of repopulating immune-deficient mice. Proc Natl Acad Sci U S A May 13;1997 94(10):5320–5325. [PubMed: 9144235]
8. Murohara T, Ikeda H, Duan J, et al. Transplanted cord blood-derived endothelial precursor cells augment postnatal neovascularization. J Clin Invest Jun;2000 105(11):1527–1536. [PubMed: 10841511]
9. Peichev M, Naiyer AJ, Pereira D, et al. Expression of VEGFR-2 and AC133 by circulating human CD34(+) cells identifies a population of functional endothelial precursors. Blood Feb 1;2000 95(3): 952–958. [PubMed: 10648408]
10. Romanov YA, Svintsitskaya VA, Smirnov VN. Searching for alternative sources of postnatal human mesenchymal stem cells: candidate MSC-like cells from umbilical cord. Stem Cells 2003;21(1):105–110. [PubMed: 12529557]
11. Ourednik J, Ourednik V, Lynch WP, Schachner M, Snyder EY. Neural stem cells display an inherent mechanism for rescuing dysfunctional neurons. Nat Biotechnol Nov;2002 20(11):1103–1110. [PubMed: 12379867]
12. Park KI, Teng YD, Snyder EY. The injured brain interacts reciprocally with neural stem cells supported by scaffolds to reconstitute lost tissue. Nat Biotechnol Nov;2002 20(11):1111–1117. [PubMed: 12379868]
13. Fazel S, Cimini M, Chen L, et al. Cardioprotective c-kit+ cells are from the bone marrow and regulate the myocardial balance of angiogenic cytokines. J Clin Invest Jul;2006 116(7):1865–1877. [PubMed: 16823487]
14. Kocher AA, Schuster MD, Szabolcs MJ, et al. Neovascularization of ischemic myocardium by human bone-marrow-derived angioblasts prevents cardiomyocyte apoptosis, reduces remodeling and improves cardiac function. Nat Med Apr;2001 7(4):430–436. [PubMed: 11283669]
15. Miyahara Y, Nagaya N, Kataoka M, et al. Monolayered mesenchymal stem cells repair scarred myocardium after myocardial infarction. Nat Med Apr;2006 12(4):459–465. [PubMed: 16582917]
16. Hess D, Li L, Martin M, et al. Bone marrow-derived stem cells initiate pancreatic regeneration. Nat Biotechnol Jul;2003 21(7):763–770. [PubMed: 12819790]
17. Lee RH, Seo MJ, Reger RL, et al. Multipotent stromal cells from human marrow home to and promote repair of pancreatic islets and renal glomeruli in diabetic NOD/scid mice. Proc Natl Acad Sci U S A Nov 14;2006 103(46):17438–17443. [PubMed: 17088535]
18. Capoccia BJ, Shepherd RM, Link DC. G-CSF and AMD3100 mobilize monocytes into the blood that stimulate angiogenesis in vivo through a paracrine mechanism. Blood Oct 1;2006 108(7): 2438–2445. [PubMed: 16735597]
19. Jin DK, Shido K, Kopp HG, et al. Cytokine-mediated deployment of SDF-1 induces revascularization through recruitment of CXCR4+ hemangiocytes. Nat Med May;2006 12(5):557–567. [PubMed: 16648859]
20. Schatteman GC, Hanlon HD, Jiao C, Dodds SG, Christy BA. Blood-derived angioblasts accelerate blood-flow restoration in diabetic mice. J Clin Invest Aug;2000 106(4):571–578. [PubMed: 10953032]
21. Pittenger MF, Martin BJ. Mesenchymal stem cells and their potential as cardiac therapeutics. Circ Res Jul 9;2004 95(1):9–20. [PubMed: 15242981]
22. Yoder MC, Mead LE, Prater D, et al. Re-defining endothelial progenitor cells via clonal analysis and hematopoietic stem/progenitor cell principals. Blood. Oct 19;2006
23. Hess DA, Meyerrose TE, Wirthlin L, et al. Functional characterization of highly purified human hematopoietic repopulating cells isolated according to aldehyde dehydrogenase activity. Blood Sep 15;2004 104(6):1648–1655. [PubMed: 15178579]
24. Hess DA, Wirthlin L, Craft TP, et al. Selection based on CD133 and high aldehyde dehydrogenase activity isolates long-term reconstituting human hematopoietic stem cells. Blood Mar 1;2006 107(5):2162–2169. [PubMed: 16269619]

25. Storms RW, Green PD, Safford KM, et al. Distinct hematopoietic progenitor compartments are delineated by the expression of aldehyde dehydrogenase and CD34. Blood Jul 1;2005 106(1):95–102. [PubMed: 15790790]
26. Storms RW, Trujillo AP, Springer JB, et al. Isolation of primitive human hematopoietic progenitors on the basis of aldehyde dehydrogenase activity. Proc Natl Acad Sci U S A Aug 3;1999 96(16):9118–9123. [PubMed: 10430905]
27. Sahovic EA, Colvin M, Hilton J, Ogawa M. Role for aldehyde dehydrogenase in survival of progenitors for murine blast cell colonies after treatment with 4-hydroperoxycyclophosphamide in vitro. Cancer Res Mar 1;1988 48(5):1223–1226. [PubMed: 3342403]
28. Sly WS, Quinton BA, McAlister WH, Rimoin DL. Beta glucuronidase deficiency: report of clinical, radiologic, and biochemical features of a new mucopolysaccharidosis. J Pediatr Feb;1973 82(2):249–257. [PubMed: 4265197]
29. Birkenmeier EH, Davisson MT, Beamer WG, et al. Murine mucopolysaccharidosis type VII. Characterization of a mouse with beta-glucuronidase deficiency. J Clin Invest Apr;1989 83(4): 1258–1266. [PubMed: 2495302]
30. Young PP, Hofling AA, Sands MS. VEGF increases engraftment of bone marrow-derived endothelial progenitor cells (EPCs) into vasculature of newborn murine recipients. Proc Natl Acad Sci U S A Sep 3;2002 99(18):11951–11956. [PubMed: 12195016]
31. Freeman BJ, Roberts MS, Vogler CA, Nicholes A, Hofling AA, Sands MS. Behavior and therapeutic efficacy of beta-glucuronidase-positive mononuclear phagocytes in a murine model of mucopolysaccharidosis type VII. Blood Sep 15;1999 94(6):2142–2150. [PubMed: 10477745]
32. Snyder EY, Taylor RM, Wolfe JH. Neural progenitor cell engraftment corrects lysosomal storage throughout the MPS VII mouse brain. Nature Mar 23;1995 374(6520):367–370. [PubMed: 7885477]
33. Soper BW, Lessard MD, Vogler CA, et al. Nonablative neonatal marrow transplantation attenuates functional and physical defects of beta-glucuronidase deficiency. Blood Mar 1;2001 97(5):1498–1504. [PubMed: 11222399]
34. Soper BW, Duffy TM, Vogler CA, Barker JE. A genetically myeloablated MPS VII model detects the expansion and curative properties of as few as 100 enriched murine stem cells. Exp Hematol Nov;1999 27(11):1691–1704. [PubMed: 10560917]
35. Hofling AA, Vogler C, Creer MH, Sands MS. Engraftment of human CD34+ cells leads to widespread distribution of donor-derived cells and correction of tissue pathology in a novel murine xenotransplantation model of lysosomal storage disease. Blood Mar 1;2003 101(5):2054–2063. [PubMed: 12406886]
36. Sands MS, Birkenmeier EH. A single-base-pair deletion in the beta-glucuronidase gene accounts for the phenotype of murine mucopolysaccharidosis type VII. Proc Natl Acad Sci U S A Jul 15;1993 90(14):6567–6571. [PubMed: 8101990]
37. Meyerrose TE, De Ugarte DA, Hofling AA, et al. In vivo Distribution of Human Adipose-Derived MSC. Stem Cells. Sep 7;2006
38. Hofling AA, Devine S, Vogler C, Sands MS. Human CD34+ hematopoietic progenitor cell-directed lentiviral-mediated gene therapy in a xenotransplantation model of lysosomal storage disease. Mol Ther Jun;2004 9(6):856–865. [PubMed: 15194052]
39. Wolfe JH, Sands MS, Barker JE, et al. Reversal of pathology in murine mucopolysaccharidosis type VII by somatic cell gene transfer. Nature Dec 24-31;1992 360(6406):749–753. [PubMed: 1465145]
40. Cai J, Cheng A, Luo Y, et al. Membrane properties of rat embryonic multipotent neural stem cells. J Neurochem Jan;2004 88(1):212–226. [PubMed: 14675165]
41. Corti S, Locatelli F, Papadimitriou D, et al. Identification of a primitive brain-derived neural stem cell population based on aldehyde dehydrogenase activity. Stem Cells Apr;2006 24(4):975–985. [PubMed: 16293577]
42. Ishikawa M, Asahara T. Endothelial progenitor cell culture for vascular regeneration. Stem Cells Dev Aug;2004 13(4):344–349. [PubMed: 15345127]

43. Gallacher L, Murdoch B, Wu DM, Karanu FN, Keeney M, Bhatia M. Isolation and characterization of human CD34(−)Lin(−) and CD34(+)Lin(−) hematopoietic stem cells using cell surface markers AC133 and CD7. Blood May 1;2000 95(9):2813–2820. [PubMed: 10779426]
44. Miraglia S, Godfrey W, Yin AH, et al. A novel five-transmembrane hematopoietic stem cell antigen: isolation, characterization, and molecular cloning. Blood Dec 15;1997 90(12):5013–5021. [PubMed: 9389721]
45. Yin AH, Miraglia S, Zanjani ED, et al. AC133, a novel marker for human hematopoietic stem and progenitor cells. Blood Dec 15;1997 90(12):5002–5012. [PubMed: 9389720]
46. Bonnet D, Bhatia M, Wang JC, Kapp U, Dick JE. Cytokine treatment or accessory cells are required to initiate engraftment of purified primitive human hematopoietic cells transplanted at limiting doses into NOD/SCID mice. Bone Marrow Transplant Feb;1999 23(3):203–209. [PubMed: 10084250]
47. Adams GB, Chabner KT, Alley IR, et al. Stem cell engraftment at the endosteal niche is specified by the calcium-sensing receptor. Nature Feb 2;2006 439(7076):599–603. [PubMed: 16382241]
48. Calvi LM, Adams GB, Weibrecht KW, et al. Osteoblastic cells regulate the haematopoietic stem cell niche. Nature Oct 23;2003 425(6960):841–846. [PubMed: 14574413]
49. Danet GH, Luongo JL, Butler G, et al. C1qRp defines a new human stem cell population with hematopoietic and hepatic potential. Proc Natl Acad Sci U S A Aug 6;2002 99(16):10441–10445. [PubMed: 12140365]
50. Wang X, Willenbring H, Akkari Y, et al. Cell fusion is the principal source of bone-marrow-derived hepatocytes. Nature Apr 24;2003 422(6934):897–901. [PubMed: 12665832]
51. Bhatia M, Bonnet D, Murdoch B, Gan OI, Dick JE. A newly discovered class of human hematopoietic cells with SCID-repopulating activity. Nat Med Sep;1998 4(9):1038–1045. [PubMed: 9734397]
52. Willenbring H, Bailey AS, Foster M, et al. Myelomonocytic cells are sufficient for therapeutic cell fusion in liver. Nat Med Jul;2004 10(7):744–748. [PubMed: 15195088]
53. Kashofer K, Siapati EK, Bonnet D. In vivo formation of unstable heterokaryons after liver damage and hematopoietic stem cell/progenitor transplantation. Stem Cells Apr;2006 24(4):1104–1112. [PubMed: 16282440]
54. Quintana-Bustamante O, Alvarez-Barrientos A, Kofman AV, et al. Hematopoietic mobilization in mice increases the presence of bone marrow-derived hepatocytes via in vivo cell fusion. Hepatology Jan;2006 43(1):108–116. [PubMed: 16374873]
55. Gentry T, Foster S, Winstead L, Deibert E, Fiordalisi M, Balber A. Simultaneous isolation of human BM hematopoietic, endothelial and mesenchymal progenitor cells by flow sorting based on aldehyde dehydrogenase activity: implications for cell therapy. Cytotherapy 2007;9(3):259–274. [PubMed: 17464758]

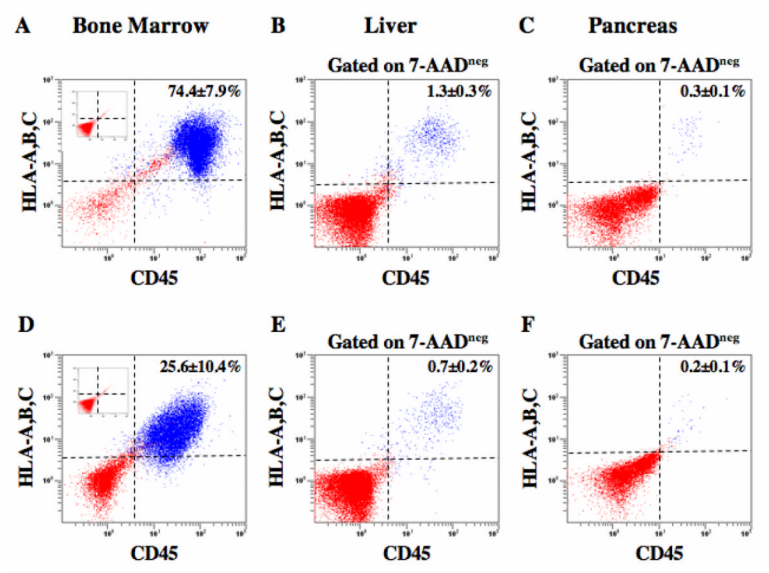

Figure 1.

FACS detection of human cells in the spleen, liver, and pancreas of transplanted NOD/SCID/MPSVII mice. Representative flow cytometric analysis of NOD/SCID/MPSVII mouse BM, liver, and pancreas after intravenous transplantation with 2×10^5 purified $ALDH^{hi}Lin^-$ (A-C), $ALDH^{hi}CD133^+Lin^-$ (D-F) cells. At 5-6 weeks post-transplantation, human hematopoietic cells were detected in mouse tissues by co-expression of human HLA-A,B,C and the human pan-leukocyte marker CD45. Mice injected with $ALDH^{hi}Lin^-$ cells showed robust repopulation in the BM (74.4±7.9%, n=4), and lower but consistent distribution in the liver (1.3±0.3%, n=4), and pancreas (0.3±0.1%, n=4). Mice transplanted with $ALDH^{hi}CD133^+Lin^-$ cells showed lower chimerism in the BM (25.6±10.4%, n=4), liver (0.7±0.2%, n=4), and pancreas (0.2±0.1%, n=4) compared with $ALDH^{hi}Lin^-$ cells. Human donor cells were not detected in mice transplanted with $ALDH^{lo}Lin^-$ (n=3, Inset 1A) or $ALDH^{hi}CD133^-Lin^-$ cells (n=3, inset 1D).

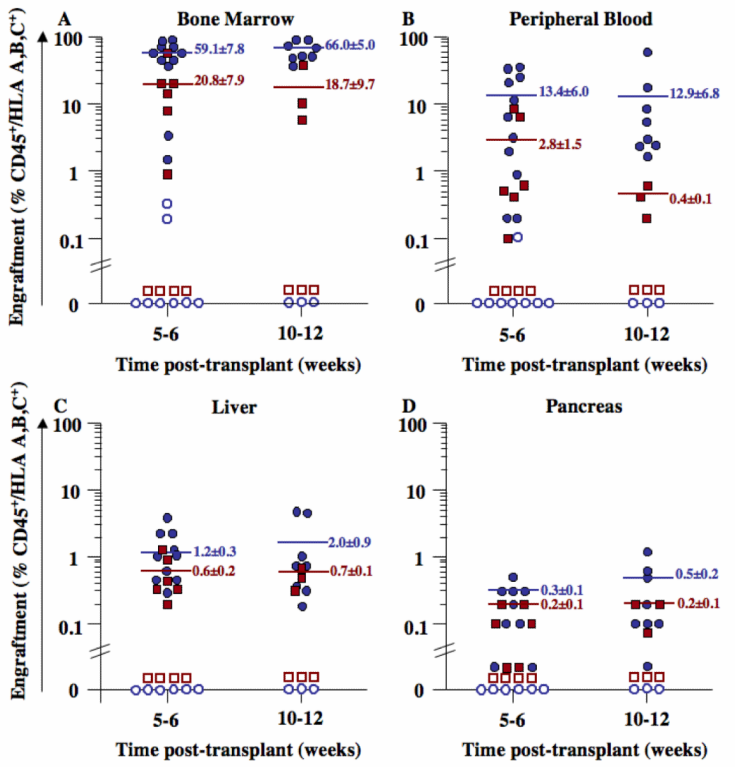

Figure 2. Summary of human cell distribution in transplanted NOD/SCID/MPSVII mice

The BM (**A**), peripheral blood (**B**), liver (**C**), or pancreas (**D**) of NOD/SCID/MPSVII mice transplanted intravenously with 0.5-4×10^5 purified $ALDH^{hi}Lin^-$ (●, n=19), $ALDH^{lo}Lin^-$ (○, n=11), $ALDH^{hi}CD133^+Lin^-$ (■, n=9), or $ALDH^{hi}CD133^-Lin^-$ (□, n=7) cells were analyzed by FACS. Human cells were detected by co-expression of human HLA-A,B,C and CD45. Transplanted $ALDH^{hi}Lin^-$ cells consistently produced a higher frequency of human progeny in the BM, peripheral blood, liver, and pancreas, as compared to $ALDH^{hi}CD133^+Lin^-$ cells ($p<0.05$). Human cells were not observed in any peripheral tissues after the transplantation of $ALDH^{lo}Lin^-$ or $ALDH^{hi}CD133^-Lin^-$ cells.

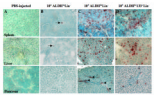

Figure 3. Donor-derived GUSB^{+} cells in the spleen, liver, and pancreas of transplanted NOD/SCID MPSVII mice

Spleen, liver, and pancreas sections from a NOD/SCID MPSVII mouse 5-6 weeks after intravenous transplantation with 10 [6] ALDH^{lo}Lin^{-} (**A**), 10^{5} ALDH^{hi}Lin^{-} (**B**), 10 [5]ALDH^{hi}CD133^{+}Lin^{-} (**C**) were analyzed for GUSB expression (ASBI staining, red) and counterstained using methyl-green (magnification 200×). Single GUSB-expressing cells were rarely detected in the spleen and liver (arrows), and were not detected in the pancreas after transplantation of ALDH^{lo}Lin^{-} cells. GUSB^{+} cells were not detected in tissues after transplantation of up to 4×105 ALDH^{hi}CD133^{-}Lin^{-} cells (not shown). Transplantation of ALDH^{hi}Lin^{-} or ALDH^{hi}CD133^{+}Lin^{-} cells produced widespread detection of GUSB^{+} cells throughout the spleen, the liver, and adjacent to ductal regions of the pancreas (arrowheads).

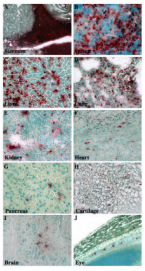

Figure 4. Widespread tissue distribution of transplanted human ALDH^{hi}Lin^{-} cells in NOD/SCID MPSVII mice

Tissue sections from a representative NOD/SCID MPSVII mouse 5-6 weeks after intravenous transplantation with 2×10^5 ALDH^{hi}Lin^{-} cells were analyzed for GUSB-expression (ASBI staining, red. magnification 200×). Donor derived GUSB^{+} cells were abundant in hematopoietic tissues such as the sternum marrow (**A**), and spleen (**B**), whereas solid bone showed less staining, with occasional positive cells. Human cells uniformly infiltrated highly perfused tissues such as the liver (**C**), and lung (**D**), at high frequencies. The kidney (**E**), heart (**F**), pancreas (**G**), and cartilage (**H**) showed consistent, but comparatively lowered detection of GUSB^{+} cells. GUSB+ human cells were also detected in the brain (**I**), and were closely associated with the retinal pigment epithelial layer of the eye (**J**). Similar tissue distribution was observed after transplantation with ALDH^{hi}CD133^{+}Lin^{-} cells.

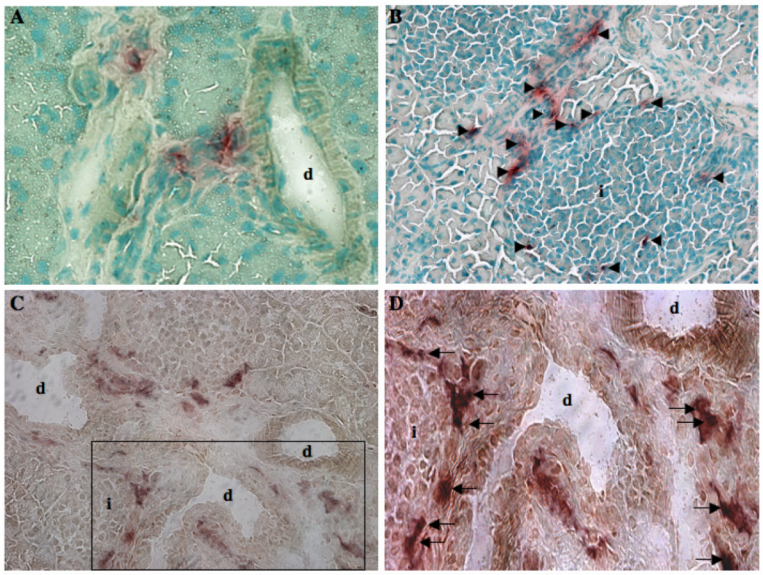

Figure 5. Human hematopoietic cells distributed to pancreatic duct and islet regions

Pancreatic sections from representative NOD/SCID/MPSVII mice 10-12 weeks after intravenous transplantation with 1-4×10^5 $ALDH^{hi}Lin^-$ cells were analyzed for GUSB-expressing cells (ASBI staining, red) with nuclei counterstained using methyl-green (magnification 100-200×). Donor-derived $GUSB^+$ cells displayed patterned distribution adjacent to acinar ducts (**A**), and surrounding islets (arrowheads, **B**). Peri-islet cells were commonly found adjacent to ductal regions. (**C, D**). Co-localization of GUSB activity (ASBI, red), and human pan-leukocyte CD45 (brown) confirmed that donor-derived $GUSB^+$ cells detected within the pancreas were primarily hematopoietic ($CD45^+$) in origin (arrows).

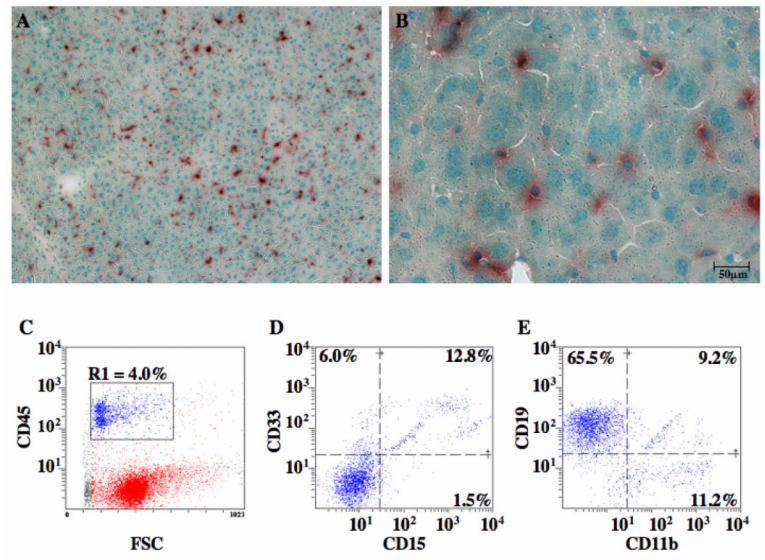

Figure 6. Hematopoietic cells distributed to the liver demonstrated GUSB and human hematopietic cell surface marker expression

Liver sections from mice injected with 2×10^5 ALDH^{hi}Lin$^-$ (**A, B**), were analyzed at 5-6 weeks post-transplantation for the presence of GUSB activity. Low power photomicrograph (A, 100×) demonstrated the widespread distribution of donor GUSB+ cells. High power photomicrograph (B, 400×) demonstrated the variable morphology and size of cells donor cells dispersed throughout the liver tissue. (**E-G**) FACS analysis was performed on human hematopoietic cells (CD45$^+$, R1) distributed in the liver at 5-6 weeks post-transplantation. Hematopoietic cells co-expressed mature lineage markers for myeloid cells (CD33, CD15), B-lymphocytes (CD19), and macrophages (CD11b)(n=3).

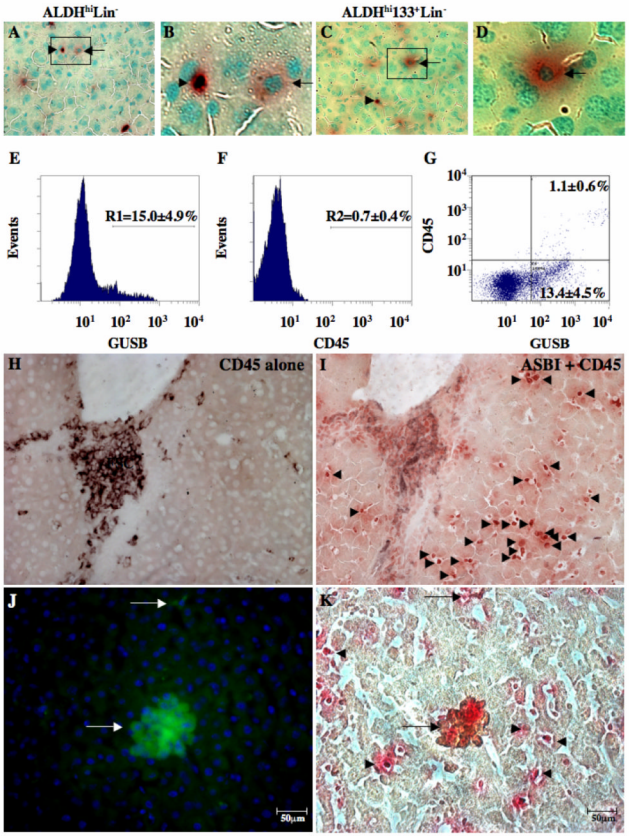

Figure 7. Donor cells engrafting the liver demonstrate variable GUSB, CD45, and hepatocyte-specific albumin expression

Liver sections from mice injected with 2×10^5 ALDH^{hi}Lin$^-$ (**A, B**), or 2×10^5 ALDH^{hi}CD133$^+$Lin$^-$ cells (**C, D**) contained small, dark red stained GUSB$^+$ cells (arrowheads) and larger, more diffusely stained cells with typical hepatocyte morphology (arrows). (**E-G**) Human donor cells were detected using a fluorescent substrate of GUSB and human pan-leukocyte marker CD45 antibody at 10-12 weeks post-transplantation. GUSB^{hi} cells (**E**) were detected at 15.0±4.9% (R1) of total cells (n=3), whereas human CD45 (**F**) was expressed at only 0.7±0.4% (R2) of total cells (n=3). (**G**) Using dual color FACS, all human CD45$^+$ cells also showed high GUSB fluorescent intensity (GUSB^{hi}) and represented 1.1±0.6% of total cells (n=3). The remainder of GUSB-expressing cells displayed lowered fluorescence intensity and did not express human CD45 (13.4±4.5%, n=3). (**H, I**) Histochemical staining for GUSB activity (ASBI, red), and CD45 expression (brown) confirmed the presence of numerous GUSB$^+$ cells that were negative for CD45 cell surface expression (arrowheads). (**J, K**) Co-staining for human hepatocyte-specific albumin using immunofluorescence and GUSB-expression using immunohistochemistry performed on liver resident donor cells revealed the presence of rare clusters and individual human cells that possess a typical hepatocyte function (arrows). The majority of donor derived GUSB$^+$ human cells did not co-stain for human albumin (arrowheads, n=3).